ZANCO Journal of Pure and Applied Sciences

TYPE Original article
DOI http://dx.doi.org/10.21271/ZJPAS.37.5.1

OPEN ACCESS

*Corresponding author
Shang Z. Abdulqadir
Shang.abdulqadir@su.edu.krd

RECEIVED :24 /02 /2025
ACCEPTED :01/06/ 2025
PUBLISHED :31/ 10/ 2025

KEYWORDS:
Nickel Nanoparticles, Lung, Pulmonotoxicity, Pulmotoxicity, Oxidative Stress, Rats..

Pulmonary toxic responses to intraperitoneal administration of nickel nanoparticles in male rats

Shang Z. Abdulqadir

Department of Biology, College of Science, Salahaddin University-Erbil, Erbil, Kurdistan Region, Iraq

ABSTRACT

The harmful effects of different levels of Nickel nanoparticles (Ni-NPs) (particle size = 20nm) on male rats' lungs were explored in the study. Intraperitoneal injection of Ni-NPs occurred at 0, 5, 20, and 100mg/kg/bw over 28 days. The quantity of malondialdehyde (MDA). The evaluation also included the levels of reduced glutathione (GSH) and the activity of antioxidant enzymes, including superoxide dismutase (SOD), glutathione peroxidase (GPX), and catalase (CAT). Additionally, observations were made on lung changes at the histopathological, immunological, and ultrastructural levels. Lung homogenates displayed a noticeable increase in MDA levels, which was dependent on the dosage. Dose-dependent changes were observed in the biochemical parameters. Histological analysis revealed several abnormalities in the rats treated with Ni-NPs, including thickening of alveolar walls. Pulmonary vessels experience blood congestion, lung parenchyma is severely damaged, and lung tissues suffer from hemorrhage. The diffuse appearance of the inflammatory leukocytes stood out as the most evident histopathological characteristic. A dose-dependent pattern was observed in all of these histopathological features. The p53 immunohistochemical demonstration exhibited a higher reaction intensity compared to the control. Examination of the ultrastructure showed that exposure to Ni-NPs led to damage in the mitochondria. The detected biochemical, histological, immunohistochemical, and ultrastructural alterations in the rat lungs demonstrate the harmful effects of NiNPs on lung health. These effects seem to be mediated in large part by the production of oxidative stress.

1.Introduction

Nanotechnology is an emerging field with diverse applications in energy, medicine, and industry (Allhoff *et al*., 2009). Materials with a size below 100 nm are classified as nanoparticles (NPs) (Laurent *et al.*, 2008). Nickle oxide nanoparticles (NIO-NP), finds extensive industrial applications such as alkaline battery cathodes, catalysis, electromagnetic devices, and pigments for ceramics and glass (Oukarroum *et al*., 2017). Oil refineries or dusts can be sources of nickel nanoparticle (NiNPs) production and harvesting. It can be emitted into the atmosphere as a byproduct of oil refineries and is harmful to the lungs of individuals living near industrial plants that utilize Ni-NP. Ni-NP can also react with chromium (Cr), manganese (Mn), and iron (Fe) to form hazardous complex compounds that pose health risks to the population (Shoeb *et al*., 2017).

Metal NPs, particularly NiNPs, have the ability to emit metal ions that are hazardous to aquatic life (Boran and Şaffak, 2018). The attention of numerous researchers has been on the detrimental consequences of NiNPs on human health (Kong *et al.*, 2014); however, additional research is required (Gu *et al.*, 2016). NiNPs may be more hazardous and perhaps carcinogenic than their fine counterparts, according to validated research (Magaye *et al*., 2014b, Katsnelson *et al*., 2015, Abdulqadir and Aziz, 2019b).

Previous studies demonstrated that after the giving of NPs to laboratory animals, they accumulate in the liver, kidney, spleen, brain, lung, etc. and cause various unfavourable influences (Borm and Kreyling, 2004, Lasagna-Reeves *et al.*, 2010, Abdulqadir and Aziz, 2019a, Abdulqadir and Aziz, 2019b). Histopathological examinations demonstrated that alveolar macrophages ingested NiO, that these macrophages deteriorated and necrosed, and that there were inflammatory reactions (Cao *et al*., 2016, Senoh *et al.*, 2017). Nevertheless, the inhalation approach is the most realistic simulation model since it most closely mimics real-world human exposure; other suitable models should be evaluated (Li *et al.*, 2018). The aims of the present work were: (1) studying the effect of different doses of 20nm NiNPs on the lung of male rats. (2) Finding the relation of such histological alterations with induced oxidative stress.

2. Material and Methods

2.1. Materials

The 20nm NiNPs powder was provided by Sigma-Aldrich Co. in .St Louis, MO, USA. The remaining lab-grade chemicals were used as they came. Analytical grade reagents have been used from the same company to satisfy the remaining requirements.

2.2. Preparation and Ultrasonication of NiNPs

Different doses of NiNPs were prepared in normal saline, specifically at 5, 20, and 100 mg/kg/bw. Using an ultrasonic homogenizer (model 150VT, manufactured by biologica, Ink, Manassas, Virginia, USA), NiNPs were sonicated for 30 seconds to obtain a suspension in normal saline (10mg/mL). The NiNPs were vibrated for 2 minutes before the injection (Tripathi *et al*., 2015).

2.3. Experimental animals

Prior to the experiments, male Wistar rats (weighing about 200-220g) were acclimated for one week. The rats were given water freely and fed commercial pellet feed. The rats were procured from Iraq's Duhok University, College of Medicine's animal house. Stainless steel mesh cages were used to house the animals, allowing them to freely access pellets and tap water. With an average relative humidity of 35% and an average temperature of 21°C±2°C, the rats were kept in the housing room.

To randomly divide twenty healthy mature male rats, four groups were formed with five rats each. Normal saline was injected into the control group rats, whereas groups 2, 3, and 4 were given ultrasonicated NiNPs suspensions at doses of 5, 20, and 100 mg/kg/bw, respectively. Over a period of four weeks, injections were administered to all groups on a five-day-a-week basis. After the final injection, the rats were euthanized, and their lung was collected for

histological, biochemical, and Immunohistochemical studies. All trials were conducted according to approved protocols by the animal care ethical committee at Salahaddin University's College of Science in Erbil, Iraq.

2.4. Biochemical assays

A portable glass homogenizer was used to homogenize the lung parts of each rat in 20 mM phosphate buffer (pH = 7.4) after they were cleaned with ice-cold normal saline solution. Using Beckman J2-21, the homogenates were subjected to a 10-minute centrifugation at 4,000 g and 4°C. The gathered supernatants were kept at -80˚C until they were ready for analysis. Spectrophotometric analysis was used to determine the level of malondialdehyde (MDA) in liver homogenate using thiobarbituric acid (TBA) solution. In summary; 150µl supernatant was combined with the following: 1ml of 17.5% trichloroacetic acid (TCA), 1ml of 0.66% TBA, mixed thoroughly by vortexing, heated in boiling water for 15 minutes, and then cooled. Following the addition of 1 ml of 70% TCA, the mixture was left to stand for 20 minutes at room temperature. Following that, it was centrifuged at 2000 rpm for 15 minutes, and the spectrophotometric analysis was performed on the resulting supernatant (Chowdhury et al., 2013).

Commercial assay kits from Elabscience Biotechnology were used to measure the levels and activities of anti-oxidative enzymes (SOD, GPX, GSH, and CAT).

2.5. Histopathological analysis

The lung sections were soaked in 10% buffered formaldehyde for 24 hours. Subsequently, they were dehydrated using ethanol at progressively higher concentrations (50%, 70%, 95%, and 100%). Finally, they were submerged in xylene, infiltrated, and embedded in paraffin wax. Using a rotary microtome (Bright, MIC), slices five micrometers thick were obtained, and hematoxylin and eosin (H&E) was used to stain them (Kiernan, 2015).

2.6. Immunohistochemical Analysis

The detection of p53 was performed using immunohistochemical kits manufactured by Leica Biosystems Newcastle Ltd., in conjunction with an automated immunostainer (AutostainerLink48 DAKO, Agilent).

2.7. Dynamic Light Scattering (DLS):

Karolinska Institute in Sweden utilized DLS to measure the size of the NiNPs.

2.8. Scanning Electron Microscopy (SEM) preparation

The SEM stub was used to mount and dry the NiNPs suspension for morphology examination, followed by platinum metal coating. SEM (SEI 450, Soran University, Kurdistan region, Iraq) was used to examine the resulting sample (Magaye et al., 2014b).

2.9. Ultrathin and Semithin Sections Preparation

The fixation process for lung samples (≤ 1mm3) during the preparation of plastic semithin sections involved immersing them in 2.5% glutaraldehyde in 0.1M cacodylate buffer pH 7.2 - 7.4 for 24 hours. The samples underwent washing in a 0.1M cacodylate buffer after fixation, then were postfixed in 1% osmium tetroxide, dehydrated with varying concentrations of ethanol (50%, 70%, 95%, and 100%), and finally cleared with propylene oxide. To examine the plastic blocks under light microscopy, they were sliced into semithin sections (0.5µm) using an ultramicrotome (Riechert Co.) and stained with 1% toluidine blue in 1% borax. The lung's ultrathin sections were captured using the JEOL JEM 1400 TEM (Janecek and Kral, 2016).

4. Statistical analysis

The statistical analysis was performed using SPSS version 22, a commonly used program. The data is reported as means ± standard error (M ± SE). A one-way analysis of variance (ANOVA) was used to test the significance of a treatment effect, and group comparisons were made using Duncan's multiple range comparison tests. Significance was attributed to p-values below 0.05.

5. Results

The current investigation trialed the effect of different NiNP doses (0, 5, 20 and 100mg/kg) on male rat lungs. The shape and size as revealed by SEM and DLS of the NiNPs is shown in Figure 1. The size of 20nm was very close to that declared by the manufacturer. This finding is

supported by other investigators (Bai et al., 2010, Sharma et al., 2009, Ahamed et al., 2010).

The presence of nanoparticles leads to elevated intracellular Reactive oxygen species' (ROS) levels, resulting in membrane lipid peroxidation (LPO) (Oberdörster *et al*., 2007). Our examination of the membrane LPO in response to Ni NPs aimed to enhance our understanding of oxidative stress processes. The level of MDA increased significantly after the NP administration and with increasing dosage of Ni NPs in comparison to the control, as shown in Figure 2. In a dose-dependent manner, the lung experienced a decrease in antioxidant enzymes superoxide dismutase (SOD), glutathione peroxidase (GPX), glutathione (GSH), and catalase (CAT).

Histologically, lung sections of rats in the control group showed a normal appearance of the lung, especially the air sac capacity (figure 2). In groups treated with NiNPs for 28 days, the lung sections demonstrated histopathological lesions such as enlargement of some air spaces, and aggregation of infiltrated lymphocytes in a dose-dependent pattern (Figure 3B-D) in which the highest dose (100mg/kg) has led to congestion and hemorrhage of air spaces (Fig. 3D). The plastic semi-thin sections revealed thickening of the interalveolar septa more clearly (Figure 4).

The data revealed that apoptosis, identified by p53-positive cells, was the predominant form of cell death. This mechanism of cell death was strongly induced at the lowest dose (5mg/kg) and declined in intensity dose-dependently. It has been discovered that modalities of cell death upon exposure to NiNPs, whether apoptosis or necrosis, are related to the amount of the dose given to the animal; smaller doses promote apoptosis, whereas higher doses produce necrosis (Ahamed, 2011). Such differences were found to be linked with the arresting mechanism of cell cycle (Levine and Oren, 2009) by p53, which is able to induce senescence and initiate apoptosis (Taylor and Stark, 2001).

The ultrastructural investigation showed mitochondrial damage as a response to NiNPs treatment (Fig. 6).

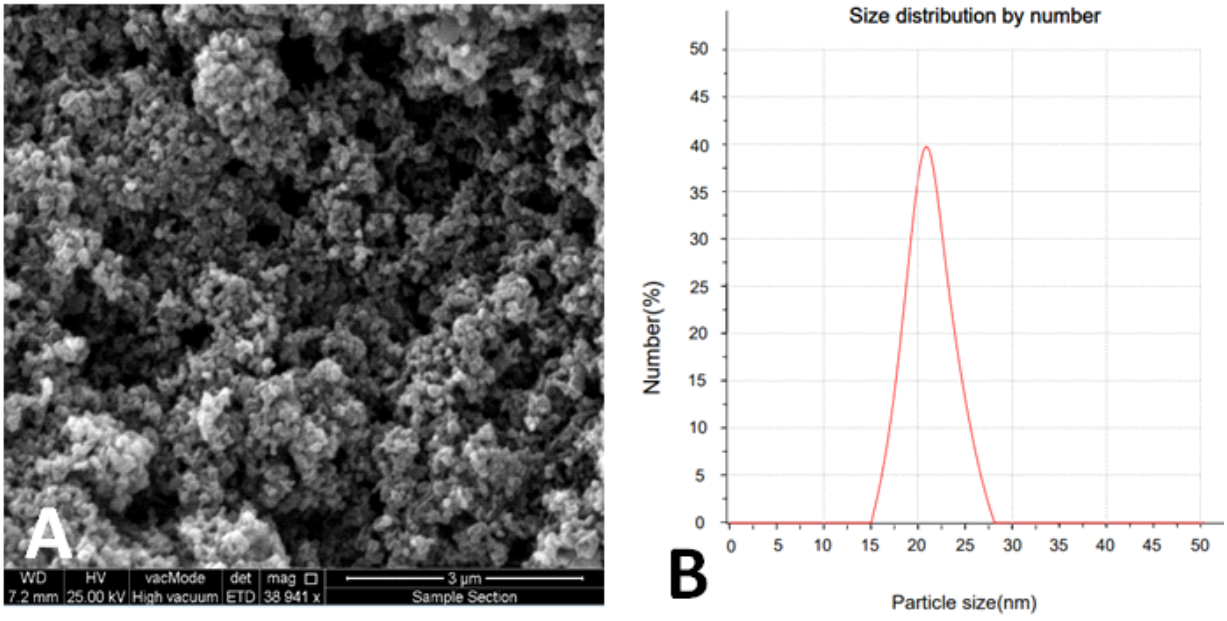

Figure 1: NiNPs shape and size as revealed by A) Scanning electron microscopy, B) Dynamic light scattering.

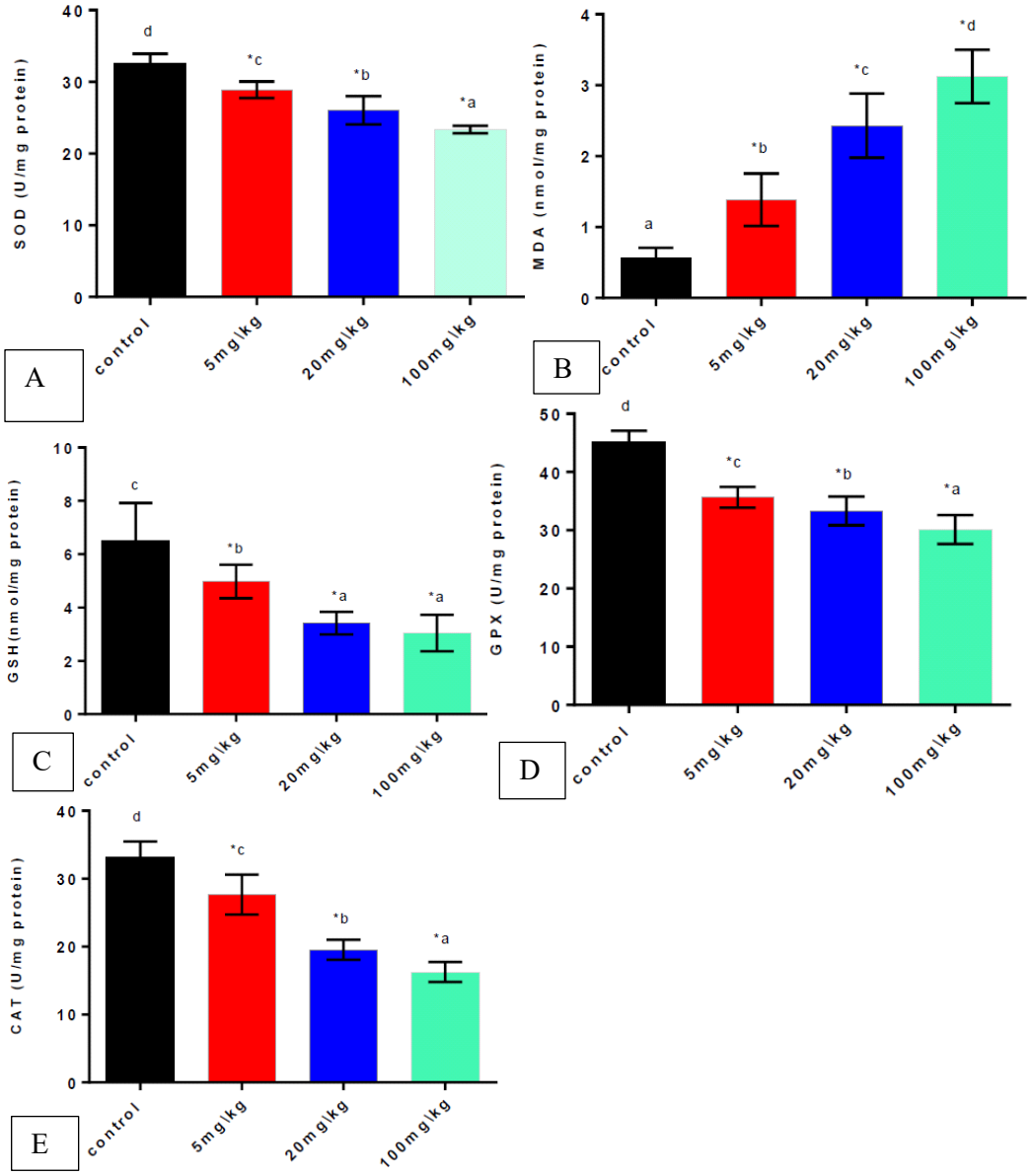

Figure 2: Evaluation of SOD (A), MDA (B), GSH (C), GPX (D) and CAT (E) after administration of different doses of NiNPs (0, 5, 20 and 100mg/Kg) in rat lung homogenate. Each value is a mean of 5 rats ±SE; a,b,c values are not sharing superscripts letters (a, b, c) differ significantly at$P \leq 0.05$. * is significant at $P \leq 0.05$

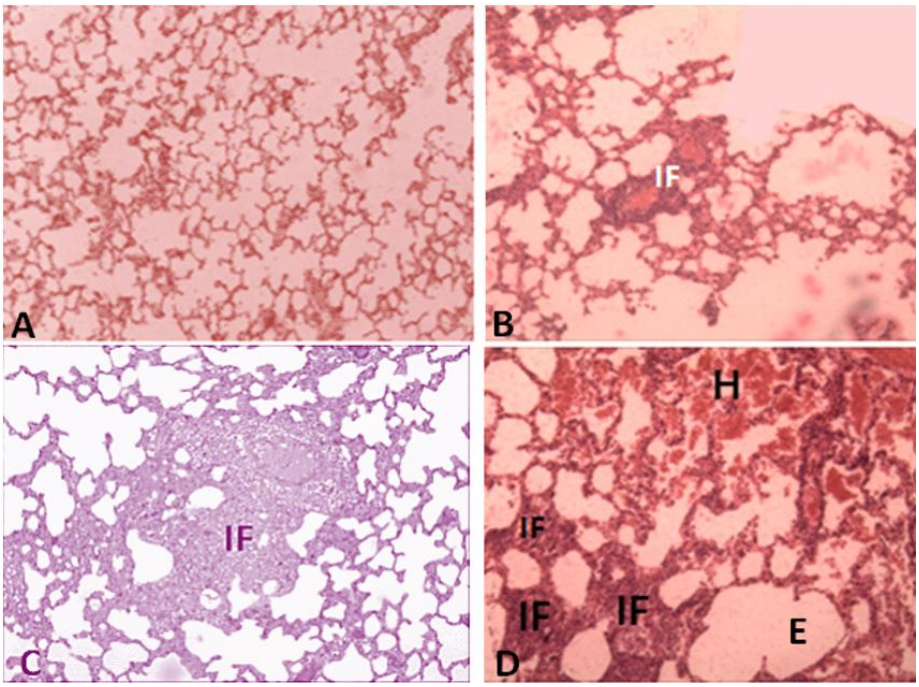

Figure 3: Sections through the lung of different doses (0.5,20 and 100mg/Kg) of NiNPs treated rats showing dose dependent toxic effect through the density of inflammatory infiltrated leucocytes aggregations (IF) within lung tissues, hemorrhage (H) and the dilatation in the lumen of air sacs and respiratory spaces, some shows emphysema (E): (A) control group (100X), (B) 5mg/Kg (400X), (C) 20mg/Kg (400X) and (D) 100mg/Kg (400X).

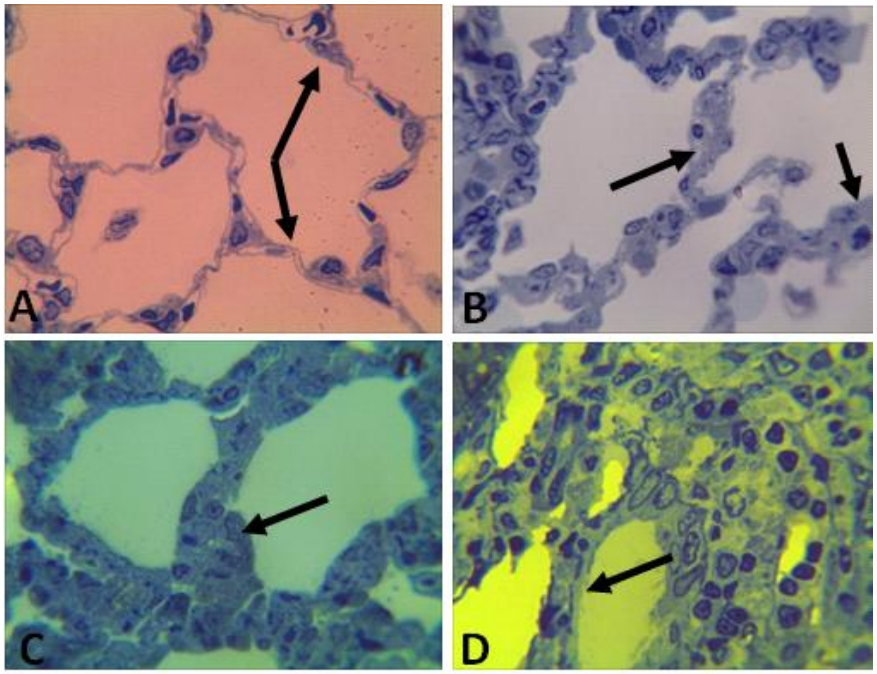

Figure 4: Plastic sections through the lung of different doses (0,5,20 and 100mg/Kg) of NiNPs treated rats. (A) Control group with normal air sacs and interalveolar septa (arrow), (B) 5mg/kg NiNPs treated group with dilated air sac (S) and thickened interalveolar septa (arrow), (C)20mg/kg treated rat lung with more air sacs dilation, hemorrhage and inflammation (arrow), (D) 100mglkg treated group appeared with high air sacs dilation, inflammation and hemorrhage (arrow), All mag=1000X.

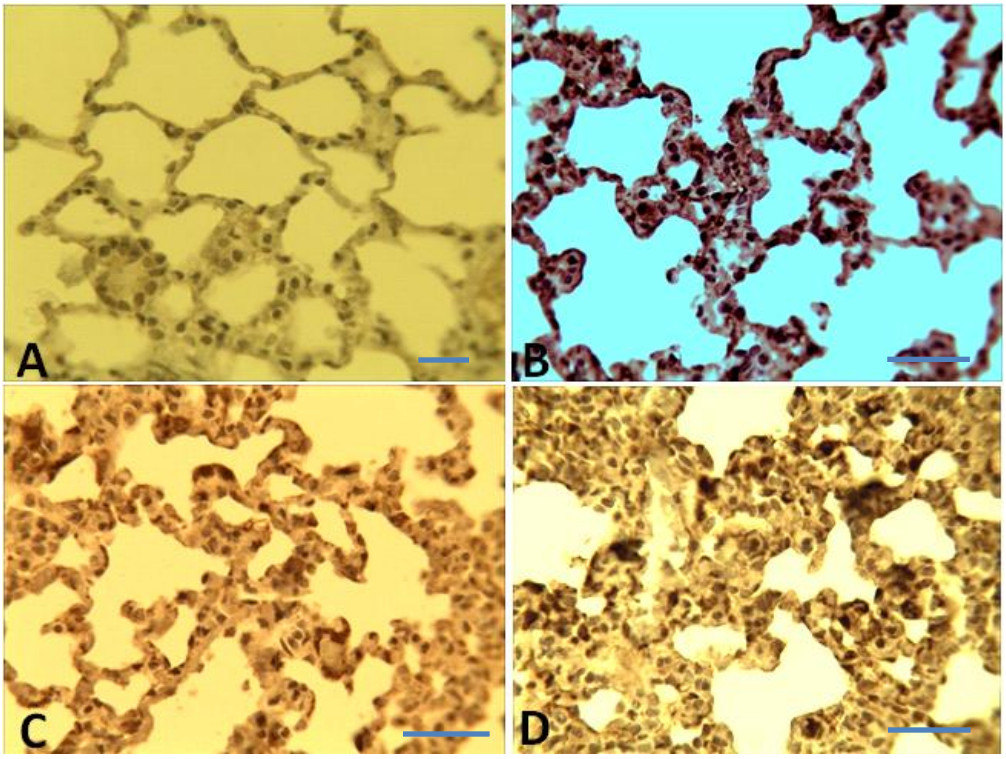

Figure 5: Immunhistochemical images of the lung of rats exposed to different doses (0,5,20 and 100mg/Kg) of NiNPs showing dose dependent positive reaction of p53 in the NiNPs treated groups compared to the negative reaction of the control (being the more reaction in the lower dose)., (A) Control group, B-D) NiNPs treated group. All mag = 400X

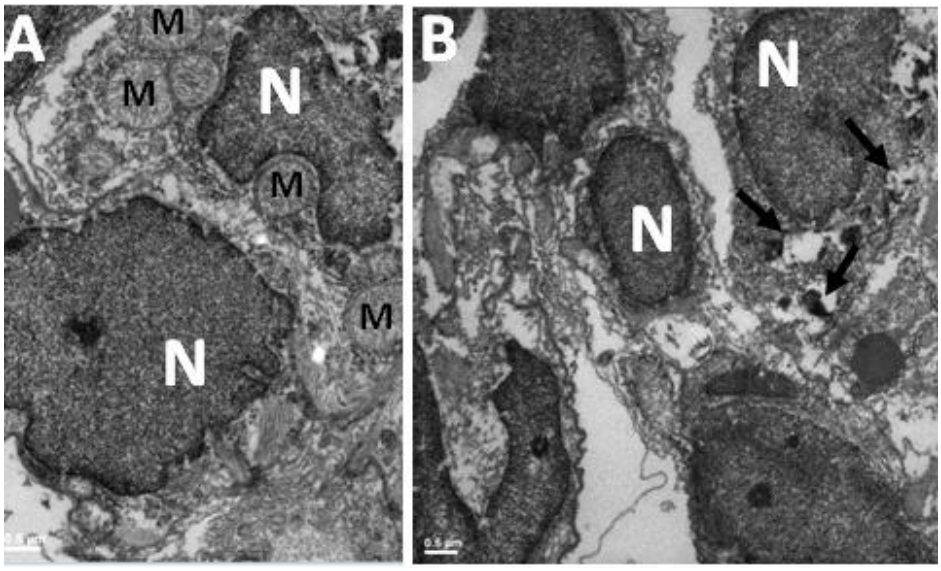

Figure 6: Electronmicrographs of rat lung showing the effect of NiNPs doses on the ultrastructure of the cells. A) Control group showing healthy mitochondria (M), B) Damage of mitochondria in the dose (20mg/Kg), M: healthy mitochondria, arrows: damaged mitochondria, N; nucleus.

6. Discussion

Over time, Ni has been incorporated into a diverse range of consumer and commercial items, ranging from guitar strings and magnets to coins, stainless steel, and rechargeable batteries (Chen et al., 2003, Kasprzak et al., 2003, M'Bemba-Meka et al., 2005). NiO NPs are known to cause various acute and chronic inflammatory

responses in the lung. One of the acute inflammatory responses of NiO NPs in the lung is neutrophilic inflammation. Previous animal studies reported acute neutrophilic or eosinophilic pulmonary inflammation with the instillation of NiO NPs in the lung. NiO NPs induced persistent inflammation as well as increased the secretion of the proinflammatory cytokines such as IL-1β and MCP-1 and tissue infiltration of macrophages and neutrophils (Sager *et al*., 2016). A neutrophilic inflammatory response of nanoparticles was associated with surface reactivity, such as ROS generation. Nanoparticle-mediated ROS generation is known as one of the main mechanisms related to inflammation in the lung (Jeong et al., 2016, Han et al., 2012). Nonetheless, noteworthy research has demonstrated the harmful consequences of nano-scale Ni and Ni-compounds on the environment and human well-being. (Kasprzak *et al*., 2003, Hao *et al*., 2006, Duman and Ozturk, 2010).

The physicochemical properties of Ni, as well as other materials, change when it is transformed from normal scale to nano-scale. The high surface area to volume ratio of NPs leads to their distinct physicochemical features. The presence of a greater number of surface atoms in comparison to bulk particles contributes to their heightened reactivity. With their improved properties, Ni-NPs are now being employed in catalysts, sensors, and electronics, as noted by (Zhang *et al*., 2003) and (Sivulka, 2005). Despite their extensive use in various industries, there is a significant dearth of information on the toxicity of Ni-NPs.

(Horie e*t al.,* 2016) and (Yu *et al*., 2018) found that NPs can cause oxidative stress by increasing reactive oxygen species (ROS) and reducing antioxidant enzyme activity. Earlier studies, however, used various methods of exposure, with none using intraperitoneal injection. The exceptional reactivity of NPs' specialized surface areas can facilitate the generation of ROS. According to (Fard *et al*., 2015), NPs have the ability to destroy both human and animal cells.

Researchers observed that nanoparticles caused lymphocytic infiltration in the lung and thickening of the alveolar septae (Gillespie *et al.*, 2010), (Cho *et al*., 2012), and (Magaye *et al.,* 2014a) have also Cytokine secretion as a result of NiNP exposure is responsible for the development of pulmonary inflammation (Cao et al., 2016). Neutrophils were found to be the primary mediators of inflammatory infiltration induced by NiONP, according to the results. Moreover, (Cao *et al.*, 2016) identified alveolar wall thickening following NiONP exposure.

However, certain studies suggest that exposure to NiONP causes only temporary, mild inflammation (Morimoto *et al.*, 2011). The erratic results observed in these investigations could possibly be clarified by considering the utilization of different cell types, animal models, exposure doses, dispersion statuses, and exposure periods (Sager *et al.*, 2016).

The latest data shows that apoptosis, identified by p53-positive cells, was the predominant form of cell death. This mechanism of cell death was strongly induced at the lowest dose (5mg/kg) and declined in intensity dose-dependently. It has been discovered that modalities of cell death upon exposure to NiNPs, whether apoptosis or necrosis, are related to the amount of the dose given to the animal; smaller doses promote apoptosis, whereas higher doses produce necrosis (Ahamed, 2011). Such differences were found to be linked with the arresting mechanism of the cell cycle (Levine and Oren, 2009) by p53, p53 protects mammals from neoplasia by inducing apoptosis, DNA repair and cell cycle arrest in response to a variety of stresses. p53-dependent arrest of cells in the G1 phase of the cell cycle is an important component of the cellular response to stress which is able to induce senescence and initiate apoptosis (Taylor and Stark, 2001).

The correlation between mitochondria and the development of oxidative stress could perhaps account for the observed increase in MDA in the group receiving NiNPs. Mitochondria produce an excess of reactive oxygen species (ROS) when conditions are pathological. If these ROS are not entirely eliminated, they cause oxidative stress, which oxidizes proteins, membranes, DNA, and cellular lipids, impairing normal physiological processes and finalizing in cell death (Moris et

al., 2017). Recently, ZnO nanoparticles were found able to induce the release of cytochorme c, decrease the intracellular ATP level, collapse the mitochondrial membrane potential, elevate the ROS level, inhibit total antioxidant enzyme activities and increase the Bax and Caspase 3 levels, whereas it decrease the Bcl-2 expression, leading to cell death (Wang et al., 2018).

7. Conclusions

This study highlights the detrimental impact of NiNPs on lung health, as evidenced by the observed biochemical, histopathological, immunohistochemical, and ultrastructural changes in the rat lungs. The induction of oxidative stress appears to play a crucial role in mediating these effects. Further research is needed to fully understand the long-term consequences of exposure to Ni-NPs and develop effective strategies to mitigate their adverse health effects.

Acknowledgements

The sincere cooperation of the department of biology, college of science, Salahaddin University would be greatly appreciated to fulfill the current study.

Novelty statement

With current advances in the industry, and the use of nickel nanoparticles, worries about their serious impacts on the respiratory system, especially the lungs are rising. However, many previous studies have encompassed this field, but the present study has focused on many aspects of adverse the effects of this material on pulmonary tissues. The facets embraced biochemical and enzymatic determinations, histopathological changes, immunological and inflammatory responses, and ultrastructural alterations. Hence, and based on my knowledge, it may be a novel study in this field.

8. References

ABDULQADIR, S. Z. & AZIZ, F. M. 2019a. Internalization and effects on cellular ultrastructure of nickel nanoparticles in rat kidneys. *International journal of nanomedicine*, 3995-4005.

ABDULQADIR, S. Z. & AZIZ, F. M. 2019b. Nickel nanoparticles induced nephrotoxicity in rats: influence of particle size.

AHAMED, M. 2011. Toxic response of nickel nanoparticles in human lung epithelial A549 cells. *Toxicology in Vitro,* 25, 930-936.

AHAMED, M., ALSALHI, M. S. & SIDDIQUI, M. 2010. Silver nanoparticle applications and human health. *Clinica chimica acta,* 411, 1841-1848.

ALLHOFF, F., LIN, P. & MOORE, D. 2009. *What is nanotechnology and why does it matter?: from science to ethics*, John Wiley & Sons.

BAI, W., ZHANG, Z., TIAN, W., HE, X., MA, Y., ZHAO, Y. & CHAI, Z. 2010. Toxicity of zinc oxide nanoparticles to zebrafish embryo: a physicochemical study of toxicity mechanism. *Journal of Nanoparticle Research,* 12, 1645-1654.

BORAN, H. & ŞAFFAK, S. 2018. Comparison of dissolved nickel and nickel nanoparticles toxicity in larval zebrafish in terms of gene expression and DNA damage. *Archives of environmental contamination and toxicology,* 74, 193-202.

BORM, P. J. & KREYLING, W. 2004. Toxicological hazards of inhaled nanoparticles—potential implications for drug delivery. *Journal of nanoscience and nanotechnology,* 4, 521-531.

CAO, Z., FANG, Y., LU, Y., QIAN, F., MA, Q., HE, M., PI, H., YU, Z. & ZHOU, Z. 2016. Exposure to nickel oxide nanoparticles induces pulmonary inflammation through NLRP3 inflammasome activation in rats. *International journal of nanomedicine*, 3331-3346.

CHEN, C.-Y., WANG, Y.-F., HUANG, W.-R. & HUANG, Y.-T. 2003. Nickel induces oxidative stress and genotoxicity in human lymphocytes. *Toxicology and applied pharmacology,* 189, 153-159.

CHO, W.-S., DUFFIN, R., POLAND, C. A., DUSCHL, A., OOSTINGH, G. J., MACNEE, W., BRADLEY, M., MEGSON, I. L. & DONALDSON, K. 2012. Differential pro-inflammatory effects of metal oxide nanoparticles and their soluble ions in vitro and in vivo; zinc and copper nanoparticles, but not their ions, recruit eosinophils to the lungs. *Nanotoxicology,* 6, 22-35.

CHOWDHURY, P., SOULSBY, M., PASLEY, J., MCKAY, D. & BANSAL, S. 2013. Effects of dietary soy protein on hematological and tissue oxidant/anti-oxidant levels in rats exposed to simulated microgravity. *J. Phys. Chem. Biophys,* 2013, 1-5.

DUMAN, F. & OZTURK, F. 2010. Nickel accumulation and its effect on biomass, protein content and antioxidative enzymes in roots and leaves of watercress (Nasturtium officinale R. Br.). *Journal of Environmental Sciences,* 22, 526-532.

FARD, J. K., JAFARI, S. & EGHBAL, M. A. 2015. A review of molecular mechanisms involved in toxicity of nanoparticles. *Advanced pharmaceutical bulletin,* 5, 447.

GILLESPIE, P. A., KANG, G. S., ELDER, A., GELEIN, R., CHEN, L., MOREIRA, A. L., KOBERSTEIN, J., TCHOU-WONG, K.-M., GORDON, T. & CHEN, L. C. 2010. Pulmonary response after exposure to inhaled nickel hydroxide nanoparticles: short and long-term studies in mice. *Nanotoxicology,* 4, 106-119.

GU, Y., WANG, Y., ZHOU, Q., BOWMAN, L., MAO, G., ZOU, B., XU, J., LIU, Y., LIU, K. & ZHAO, J. 2016. Inhibition of nickel nanoparticles-induced toxicity by

epigallocatechin-3-gallate in JB6 cells may be through down-regulation of the MAPK signaling pathways. *PloS one,* 11**,** e0150954.

HAN, X., CORSON, N., WADE-MERCER, P., GELEIN, R., JIANG, J., SAHU, M., BISWAS, P., FINKELSTEIN, J. N., ELDER, A. & OBERDÖRSTER, G. 2012. Assessing the relevance of in vitro studies in nanotoxicology by examining correlations between in vitro and in vivo data. *Toxicology,* 297**,** 1-9.

HAO, F., WANG, X. & CHEN, J. 2006. Involvement of plasma-membrane NADPH oxidase in nickel-induced oxidative stress in roots of wheat seedlings. *Plant Science,* 170**,** 151-158.

HORIE, M., YOSHIURA, Y., IZUMI, H., OYABU, T., TOMONAGA, T., OKADA, T., LEE, B.-W., MYOJO, T., KUBO, M. & SHIMADA, M. 2016. Comparison of the pulmonary oxidative stress caused by intratracheal instillation and inhalation of NiO nanoparticles when equivalent amounts of NiO are retained in the lung. *Antioxidants,* 5**,** 4.

JANECEK, M. & KRAL, R. 2016. *Modern electron microscopy in physical and life sciences*, BoD–Books on Demand.

JEONG, J., KIM, J., SEOK, S. H. & CHO, W.-S. 2016. Indium oxide (In 2 O 3) nanoparticles induce progressive lung injury distinct from lung injuries by copper oxide (CuO) and nickel oxide (NiO) nanoparticles. *Archives of toxicology,* 90**,** 817-828.

KASPRZAK, K. S., SUNDERMAN JR, F. W. & SALNIKOW, K. 2003. Nickel carcinogenesis. *Mutation Research/Fundamental and Molecular Mechanisms of Mutagenesis,* 533**,** 67-97.

KATSNELSON, B. A., PRIVALOVA, L. I., SUTUNKOVA, M. P., GURVICH, V. B., LOGINOVA, N. V., MINIGALIEVA, I. A., KIREYEVA, E. P., SHUR, V. Y., SHISHKINA, E. V. & BEIKIN, Y. B. 2015. Some inferences from in vivo experiments with metal and metal oxide nanoparticles: the pulmonary phagocytosis response, subchronic systemic toxicity and genotoxicity, regulatory proposals, searching for bioprotectors (a self-overview). *International Journal of Nanomedicine***,** 3013-3029.

KIERNAN, J. 2015. *Histological and histochemical methods*, Scion publishing ltd.

KONG, L., TANG, M., ZHANG, T., WANG, D., HU, K., LU, W., WEI, C., LIANG, G. & PU, Y. 2014. Nickel nanoparticles exposure and reproductive toxicity in healthy adult rats. *International journal of molecular sciences,* 15**,** 21253-21269.

LASAGNA-REEVES, C., GONZALEZ-ROMERO, D., BARRIA, M., OLMEDO, I., CLOS, A., RAMANUJAM, V. S., URAYAMA, A., VERGARA, L., KOGAN, M. J. & SOTO, C. 2010. Bioaccumulation and toxicity of gold nanoparticles after repeated administration in mice. *Biochemical and biophysical research communications,* 393**,** 649-655.

LAURENT, S., FORGE, D., PORT, M., ROCH, A., ROBIC, C., VANDER ELST, L. & MULLER, R. N. 2008. Magnetic iron oxide nanoparticles: synthesis, stabilization, vectorization, physicochemical characterizations, and biological applications. *Chemical reviews,* 108**,** 2064-2110.

LEVINE, A. J. & OREN, M. 2009. The first 30 years of p53: growing ever more complex. *Nature reviews cancer,* 9**,** 749-758.

LI, Y.-S., OOTSUYAMA, Y., KAWASAKI, Y., MORIMOTO, Y., HIGASHI, T. & KAWAI, K. 2018. Oxidative DNA damage in the rat lung induced by intratracheal instillation and inhalation of nanoparticles. *Journal of Clinical Biochemistry and Nutrition,* 62**,** 238-241.

M'BEMBA-MEKA, P., LEMIEUX, N. & CHAKRABARTI, S. K. 2005. Nickel compound-induced DNA single-strand breaks in chromosomal and nuclear chromatin in human blood lymphocytes in vitro: role of oxidative stress and intracellular calcium. *Mutation Research/Genetic Toxicology and Environmental Mutagenesis,* 586**,** 124-137.

MAGAYE, R., ZHOU, Q., BOWMAN, L., ZOU, B., MAO, G., XU, J., CASTRANOVA, V., ZHAO, J. & DING, M. 2014a. Metallic nickel nanoparticles may exhibit higher carcinogenic potential than fine particles in JB6 cells. *PloS one,* 9**,** e92418.

MAGAYE, R. R., YUE, X., ZOU, B., SHI, H., YU, H., LIU, K., LIN, X., XU, J., YANG, C. & WU, A. 2014b. Acute toxicity of nickel nanoparticles in rats after intravenous injection. *International journal of nanomedicine***,** 1393-1402.

MORIMOTO, Y., OYABU, T., OGAMI, A., MYOJO, T., KURODA, E., HIROHASHI, M., SHIMADA, M., LENGGORO, W., OKUYAMA, K. & TANAKA, I. 2011. Investigation of gene expression of MMP-2 and TIMP-2 mRNA in rat lung in inhaled nickel oxide and titanium dioxide nanoparticles. *Industrial health,* 49**,** 344-352.

MORIS, D., SPARTALIS, M., TZATZAKI, E., SPARTALIS, E., KARACHALIOU, G.-S., TRIANTAFYLLIS, A. S., KARAOLANIS, G. I., TSILIMIGRAS, D. I. & THEOCHARIS, S. 2017. The role of reactive oxygen species in myocardial redox signaling and regulation. *Annals of translational medicine,* 5.

OBERDÖRSTER, G., STONE, V. & DONALDSON, K. 2007. Toxicology of nanoparticles: a historical perspective. *Nanotoxicology,* 1**,** 2-25.

OUKARROUM, A., ZAIDI, W., SAMADANI, M. & DEWEZ, D. 2017. Toxicity of nickel oxide nanoparticles on a freshwater green algal strain of Chlorella vulgaris. *BioMed research international,* 2017**,** 9528180.

SAGER, T., WOLFARTH, M., KEANE, M., PORTER, D., CASTRANOVA, V. & HOLIAN, A. 2016. Effects of nickel-oxide nanoparticle pre-exposure dispersion status on bioactivity in the mouse lung. *Nanotoxicology,* 10**,** 151-161.

SENOH, H., KANO, H., SUZUKI, M., OHNISHI, M., KONDO, H., TAKANOBU, K., UMEDA, Y., AISO, S. & FUKUSHIMA, S. 2017. Comparison of single or multiple intratracheal administration for pulmonary toxic responses of nickel oxide nanoparticles in rats. *journal of Occupational Health,* 59**,** 112-121.

SHARMA, V., SHUKLA, R. K., SAXENA, N., PARMAR, D., DAS, M. & DHAWAN, A. 2009. DNA damaging potential of zinc oxide nanoparticles in human epidermal cells. *Toxicology letters,* 185**,** 211-218.

SHOEB, M., KODALI, V., FARRIS, B., BISHOP, L. M., MEIGHAN, T., SALMEN, R., EYE, T., ROBERTS, J. R., ZEIDLER-ERDELY, P. & ERDELY, A. 2017. Evaluation of the molecular mechanisms associated with cytotoxicity and inflammation after pulmonary exposure to different metal-rich welding particles. *Nanotoxicology,* 11**,** 725-736.

SIVULKA, D. J. 2005. Assessment of respiratory carcinogenicity associated with exposure to metallic nickel: A review. *Regulatory Toxicology and Pharmacology,* 43**,** 117-133.

TAYLOR, W. R. & STARK, G. R. 2001. Regulation of the G2/M transition by p53. *Oncogene,* 20**,** 1803-1815.

TRIPATHI, B., PANIWNYK, L., CHERKASOV, N., IBHADON, A. O., LANA-VILLARREAL, T. & GÓMEZ, R. 2015. Ultrasound-assisted selective hydrogenation of C-5 acetylene alcohols with Lindlar catalysts. *Ultrasonics sonochemistry,* 26**,** 445-451.

WANG, W., ZENG, C., FENG, Y., ZHOU, F., LIAO, F., LIU, Y., FENG, S. & WANG, X. 2018. The size-dependent effects of silica nanoparticles on endothelial cell apoptosis through activating the p53-caspase pathway. *Environmental Pollution,* 233**,** 218-225.

YU, S., LIU, F., WANG, C., ZHANG, J., ZHU, A., ZOU, L., HAN, A., LI, J., CHANG, X. & SUN, Y. 2018. Role of oxidative stress in liver toxicity induced by nickel oxide nanoparticles in rats. *Molecular Medicine Reports,* 17**,** 3133-3139.

ZHANG, Q., KUSAKA, Y., ZHU, X., SATO, K., MO, Y., KLUZ, T. & DONALDSON, K. 2003. Comparative toxicity of standard nickel and ultrafine nickel in lung after intratracheal instillation. *Journal of occupational health,* 45**,** 23-30.